Cancer Research

Anti-Jagged Immunotherapy Inhibits MDSCs and Overcomes Tumor-Induced Tolerance

Rosa A. Sierra[1], Jimena Trillo-Tinoco[1], Eslam Mohamed[1], Lolie Yu[2], Bhagelu R. Achyut[3], Ali Arbab[3], Jennifer W. Bradford[4], Barbara A. Osborne[5], Lucio Miele[2], and Paulo C. Rodriguez[1]

Abstract

Myeloid-derived suppressor cells (MDSC) are a major obstacle to promising forms of cancer immunotherapy, but tools to broadly limit their immunoregulatory effects remain lacking. In this study, we assessed the therapeutic effect of the humanized anti–Jagged1/2-blocking antibody CTX014 on MDSC-mediated T-cell suppression in tumor-bearing mice. CTX014 decreased tumor growth, affected the accumulation and tolerogenic activity of MDSCs in tumors, and inhibited the expression of immunosuppressive factors arginase I and iNOS. Consequently, anti-Jagged therapy overcame tumor-induced T-cell tolerance, increased the infiltration of reactive $CD8^+$ T cells into tumors, and enhanced the efficacy of T-cell–based immunotherapy. Depletion of MDSC-like cells restored tumor growth in mice treated with anti-Jagged, whereas coinjection of MDSC-like cells from anti–Jagged-treated mice with cancer cells delayed tumor growth. Jagged1/2 was induced in MDSCs by tumor-derived factors via NFkB-p65 signaling, and conditional deletion of NFkB-p65 blocked MDSC function. Collectively, our results offer a preclinical proof of concept for the use of anti-Jagged1/2 to reprogram MDSC-mediated T-cell suppression in tumors, with implications to broadly improve the efficacy of cancer therapy. *Cancer Res; 77(20); 5628–38. ©2017 AACR.*

Introduction

The coordinated activity of the innate and adaptive arms of the immune system is essential to protect individuals against cancer. However, established tumors create a highly tolerogenic microenvironment that blocks the development of protective immunity (1). Myeloid-derived suppressor cells (MDSC) are primary components of the immunosuppressive tumor milieu and are emerging as a major obstacle in the successful development of promising cancer treatments (2). Therapeutic inhibition of the immunosuppressive effects induced by MDSCs in cancer patients treated with chemotherapy, radiotherapy, or immunotherapy regimens is thought to be a highly promising strategy with potentially significant clinical impact. However, current approaches to clinically inhibit MDSCs are limited to multityrosine kinase inhibitors or myelosuppressive agents that are only partially effective and cause rebounds in MDSC numbers as the bone marrow recovers (3, 4). Therefore, new therapeutic strategies to block MDSCs in cancer patients are needed. Numerous mAb-based therapies have shown promising efficacy as cancer therapeutics through the direct targeting of tumor antigens or tolerogenic molecules on immune cells (5, 6). Although several mAb-based approaches have been developed to directly target exhausted or immunosuppressed T cells in cancer patients, there are limited mAb-based therapies that could effectively inhibit MDSCs (7).

The Notch family of receptors regulates a highly conserved pathway that controls the development, differentiation, survival, and function of many cell types, including immune cells (8). Mammals have four Notch receptors (Notch1 through 4) that are bound by five ligands of the Jagged (Jagged1 and Jagged2) and the Delta-like (DLL1, DLL3, and DLL4) families (9). Binding of Notch receptors to the Jagged or DLL membrane ligands induces a two-step proteolytic activation, leading to the intracellular release and nuclear translocation of the Notch intracellular active domain (NICD). Once there, NICD binds to the recombination signal-binding protein-Jκ (RBP-Jκ) and recruits a mastermind-like (MAML1-3) coactivator, promoting the transcription of multiple genes (10). In addition, NICD triggers a number of noncanonical responses (11, 12). Binding of the Notch receptors on $CD8^+$ T cells to DLL ligands on antigen-presenting cells induces antitumor cytotoxic responses (13–15), whereas binding of Notch to Jagged members resulted in suppressive signals (16). The mechanism for this opposite effect remains unclear with possible explanations, including different kinetics of Notch activation or selectivity of DLL and Jagged ligands for Notch receptors. Although the effects of Notch signaling in innate and adaptive immune responses are the focus of active research, the mechanisms leading to the expression of Jagged molecules in tumors and the potential effect of their blockade as a cancer therapy remain largely unknown.

In this study, we aimed to test the antitumor effects of CTX014, a humanized IgG1-blocking antibody that recognizes

[1]H. Lee Moffitt Cancer Center and Research Institute, Tampa, Florida. [2]Louisiana State University Health Sciences Center, New Orleans, Louisiana. [3]Georgia Cancer Center, Augusta University, Augusta, Georgia. [4]Department of Biological Sciences, Augusta University, Augusta, Georgia. [5]Department of Veterinary and Animal Sciences, University of Massachusetts, Amherst, Massachusetts.

Note: Supplementary data for this article are available at Cancer Research Online (http://cancerres.aacrjournals.org/).

Corresponding Author: Paulo C. Rodriguez, H. Lee Moffitt Cancer Center and Research Institute, 12902 Magnolia Drive MRC-2067E, Tampa, FL, 33612. Phone: 813-745-1457; E-mail: Paulo.Rodriguez@Moffitt.org

doi: 10.1158/0008-5472.CAN-17-0357

human and mouse Jagged1 and 2. Our results show that anti-Jagged therapy triggered antitumor T-cell responses through the induction of potentially immunogenic MDSC-like cells (MDSC-LC; ref. 17). Additional findings demonstrate the role of NFκB-p65 in the upregulation of Jagged1/2 ligands in tumor-associated MDSCs. Thus, results identify a promising therapeutic tool to potentially block MDSCs in tumors, thereby addressing a major obstacle in the development of successful therapies against cancer.

Material and Methods

Cell lines and treatment of mice

3LL Lewis lung carcinoma, MCA-38 colon carcinoma, EL-4 thymoma, B16-F10 melanoma, and ovalbumin-expressing EL-4 (EG-7) cells (ATCC) were injected s.c. into mice, as described previously (18). Tumor cell lines were authenticated on May 2016 and validated to be mycoplasma-free using an ATCC detection kit in June 2016. All experiments were conducted with cells within six passages. C57BL/6 mice (6- to 8-week-old female) were purchased from Harlan-Envigo. OT-1 and recombination activating gene 1 null (Rag) mice were obtained from The Jackson Laboratories. Previously reported NFκB-p65$^{flox/flox}$ mice (19) were crossed with Lysozyme Cre^{+} (LysM-Cre) mice. Tumor-bearing mice were treated i.p. with nontoxic concentrations of the anti-Jagged antibody (CTX-014, Cytomx, 5 mg/kg, every 3 days) or isotype IgG control (BioXcell, 5 mg/kg) starting on day 6 post-tumor injection and throughout the experiment. To deplete CD8^{+} T cells or MDSC-LC, 3LL-bearing mice were pretreated 1 day before the anti-Jagged injection with 400 μg anti-CD8 (clone 53.6.72; BioXcell) or 250 μg anti–Gr-1 (clone RB6-8C5; BioXcell), respectively. Maintenance i.p. doses of depleting antibodies were given every 3rd day until tumor endpoint. In MDSC coinjection studies, 1×10^6 tumor MDSCs from 3LL-bearing mice treated with anti-Jagged or isotype control were coinjected s.c. with 1×10^6 3LL cells. Tumor volume was measured using calipers and calculated using the formula [(small diameter)^2 × (large diameter) × 0.5]. Experiments using mice were approved by the Institutional Animal Care and Use Committee of Augusta University, following the recommended guidelines.

Antibodies

Purified antibodies against arginase I (clone19), iNOS (54/iNOS), and gp91^{phox} (53/gp91), and fluorochrome-conjugated antibodies against CD8 (53-6.7), CD11b (M1/70), CD44 (IM7), CD45.1 (A20), CD45.2 (104), CD49f (GoH3), CD69 (H1.2F3), Gr-1 (RB6-8C5), XCR1 (ZET), CD103 (2E7), IFNγ (XMG1.2), and Ki-67 (16A8) were obtained from Becton Dickinson or Biolegend. Antibodies against β-actin (AC-74) and vinculin (V284) were from Sigma-Aldrich and anti-p84 (5E10) from Abcam. Polyclonal antibodies against NFκB-p65 (D14E1) and Jagged1 (28H8) were obtained from Cell Signaling Technology, whereas anti-Jagged2 (H-143) was from Santa Cruz Biotechnology.

Western blot

Cell lysates were electrophoresed in 8% Tris-Glycine gels, transferred to PVDF membranes, and immunoblotted with the corresponding primary antibodies. Membrane-bound immune complexes were detected using ECL in a Chemi-Doc imaging system (Bio-Rad). Densitometry of NFκB-p65 normalized to nuclear p84 was calculated using the Bio-Rad Image-Lab software.

Cell isolation and suppression assays

Tumors digested with DNAse and Liberase (Roche) were used to isolate different cellular populations by flow cytometry. 3LL cancer cells were recovered by sorting the CD45^{neg} CD49f^{+} cells, whereas tumor-infiltrating myeloid cells were isolated based on the expression of CD45^{+} CD11b^{+}. For functional assays, MDSCs from tumors or spleens of tumor-bearing mice or immature myeloid cells (iMC) from spleens of mice without tumors were harvested using magnetic beads, as described previously (18, 20). Purity for each population ranged from 90% to 99%, as detected by flow cytometry. Isolated MDSCs were cocultured for 72 hours with anti–CD3/CD28-activated T cells labeled with carboxyfluorescein succinimidyl ester (CFSE) and T-cell proliferation or IFNγ expression monitored by flow cytometry (14). Splenic MDSCs were cultured for 48 hours with GM-CSF (20 ng/mL) and 30% 3LL-tumor explants (TES; ref. 21) in the presence of anti-Jagged antibody (2 μg/mL).

Adoptive cellular therapy

For adoptive T-cell transfer (ACT) therapy, CD45.2^{+} mice were injected s.c. with EG-7 cells and started receiving the anti-Jagged or control treatments 6 days after tumor injection. One day later, mice received ACT with 1×10^6 negatively sorted CD45.1^{+} CD8^{+} OT-1 cells that were preactivated for 48 hours with SIINFEKL (14). Ten days later, spleens and tumors were tested for the presence of the transferred CD45.2^{neg} CD45.1^{+} CD8^{+} OT-1 cells and for the expression of IFNγ. For Elispot assays, spleens were collected 10 days after OT-1 transfer and activated with 2 μg/mL SIINFEKL for 24 hours before measuring IFNγ production.

Hematoxylin & eosin staining and immunofluorescence

Formalin-fixed and paraffin-embedded tissue sections were stained with hematoxylin & eosin (H&E) for histology. For immunofluorescence, deparaffinization and antigen retrieval were completed, and sections were blocked in 2% donkey serum and incubated overnight with rat anti-mouse CD8 (53-6.7; Novus Biologicals) or double labeled with mouse anti–pan-cytokeratin (C-11; Thermo) and rabbit anti-mouse cleaved caspase-3 (5A1E; Cell Signaling Technology), followed by washing in PBS and incubation in donkey anti-rat or anti-mouse/rabbit IgG Alexa Fluor 488/647 (Thermo Fisher Scientific). Next, sections were washed in PBS, mounted in aqueous mounting media with DAPI (Thermo-Fisher), and visualized in a Zeiss-LSM-780 Upright-Confocal microscope.

Chromatin immunoprecipitation

Chromatin immunoprecipitation (ChIP) assays were done using a SimpleChip kit (Cell Signaling Technology), following the vendor's recommendations. Briefly, digested and cross-linked chromatin was prepared from 4×10^6 tumor-MDSCs or splenic MDSCs treated or not with TES for 48 hours, followed by immunoprecipitation with antibodies against NFκB-p65, Histone H3, or rabbit IgG (Cell Signaling Technology). Eluted and purified DNA was analyzed by qPCR with prevalidated ChIP primers targeting the Jagged1 or Jagged2 promoters, purchased from Qiagen. Primers against RPL30 promoter were used as housekeeping gene control.

Quantitative RT-PCR

Total RNA was isolated from cells using TRIzol (Life Technologies). Reverse transcription was performed using the Bio-Rad iScript-cDNA synthesis Kit. Quantitative PCR was achieved on an Applied Biosystems thermocycler using Bio-Rad SYBR Green Supermix with prevalidated primers targeting mouse *Jagged1*, *Jagged2*, *Notch1*, *Notch2*, or *Hes1* (QuantiTect; Qiagen). Fold-change expression was calculated comparing the RNA values from experimental samples relative to the endogenous actin control (forward, TGTGATGGTGGGAATGGGTCAGAA; reverse, TGTGGTGCCAGATCTTCTCCATGT), compared with the results obtained from a pooled sample. Thus, fold change $=2^{-\Delta(\Delta CT)}$, where $\Delta C_T = C_{T\ (target)} - C_{T\ (actin)}$; and $\Delta(\Delta CT) = \Delta C_{T\ (target)} - \Delta CT_{\ (control,\ pool\ of\ all\ samples)}$.

Statistical analysis

Statistical analyses were performed in GraphPad Prism. Significance tests were conducted at a 5% significance level. Experimental differences between endpoints were assessed by ANOVA, whereas comparisons of mean were carried out with the Tukey procedure or the Dunnet procedure for comparisons with controls.

Results

Antitumor effects of anti-Jagged therapy

We aimed to determine the therapeutic effects of the anti-Jagged antibody in several s.c. tumor models, including 3LL, EL-4, MCA-38, and B16. Mice were treated starting on day 6 after tumor injection and continued to be injected every 3 days throughout the experiment. A significant delay in tumor growth was found in all the tested cancer models after treatment with the anti-Jagged antibody, compared with untreated mice or animals injected with the same dose of an isotype control (Fig. 1A). Also, evaluation of tumor morphology by H&E indicated that tumors from anti–Jagged-treated mice show coagulative necrosis and moderate edema, surrounded by a mild inflammatory infiltrate (Fig. 1B, left), which correlated with the coexpression of tumor cell marker, cytokeratin, and cell death marker, cleaved caspase-3 (Fig. 1B, right), and a similar distribution of vascular $CD31^+$ cells (Supplementary Fig. S1). Thus, anti-Jagged therapy induced antitumor effects and cancer cell death *in vivo* independently of changes in tumor vascularization.

In order to identify potential populations targeted by the anti-Jagged therapy, we first measured the expression of Jagged1 and 2 in tumors cultured *in vitro* and those collected from mice. A higher expression of *Jagged1* and *2* was detected in the s.c. tumors obtained from mice, compared with the cancer cells cultured *in vitro* (Fig. 1C). Consistent with these data, the anti-Jagged antibody failed to induce cytotoxicity against cultured 3LL cells (Fig. 1D). Next, we measured the expression of *Jagged1* and *2* in sorted cells representing the two most abundant populations in 3LL tumors, the 3LL cancer cells ($CD45^{neg}$ $CD49f^+$) and myeloid cells ($CD45^+$ $CD11b^+$; Supplementary Fig. S2). The elevated levels of *Jagged1* and *2* in tumors were distributed among the cancer cells and myeloid cells (Fig. 1E and F), suggesting the potential recognition of both cellular populations by anti-Jagged.

Anti-Jagged therapy affected the accumulation and function of tumor-MDSCs

Because MDSCs ($CD11b^+$ $Gr\text{-}1^+$) were one of the major cellular subsets expressing Jagged ligands in tumors (14), we tested the effect of the anti-Jagged therapy on the accumulation and function of MDSCs. Surprisingly, we found an elevated frequency of $CD11b^+$ $Gr\text{-}1^+$ cells in tumors from mice treated with anti-Jagged, compared with control mice, whereas similar percentages of these cells were noted in the spleen (Fig. 2A). Moreover, tumor-linked $CD11b^+$ $Gr\text{-}1^+$ cells from anti–Jagged-treated 3LL-bearing mice had a lower ability to block CFSE-based T-cell proliferation or IFNγ production, compared with MDSCs from control mice (Fig. 2B and C), suggesting an increase in MDSC-LC populations (17). The low tolerogenic activity of MDSC-LC from anti–Jagged-treated mice correlated with a lower expression of MDSC-suppressive mediators, iNOS and arginase I, and decreased levels of the antibody targets, Jagged1 and 2 (Fig. 2D). Interestingly, MDSC-LC from anti–Jagged-treated mice showed slightly higher levels of MDSC-regulator, $gp91^{phox}$, and similar proportions of Annexin V^+ (Fig. 2D and E), suggesting that anti-Jagged differentially modulates MDSC-regulatory pathways, without inducing apoptosis. Next, we aimed to determine the role of MDSC-LC in the antitumor effects induced by anti-Jagged. As such, we depleted MDSC-LC in tumor-bearing mice treated with anti-Jagged using an anti–Gr-1 antibody (Supplementary Fig. S3), or coinjected MDSC-LC from anti–Jagged-treated mice with 3LL tumors. Results show that elimination of MDSC-LC restored tumor growth in mice treated with anti-Jagged (Fig. 2F), whereas coinjection of 3LL cells with MDSC-LC from anti–Jagged-treated mice, but not isotype-treated animals, resulted in delayed tumor growth (Fig. 2G). Taken together, data suggest that treatment of tumor-bearing mice with anti-Jagged induces the accumulation of potentially antitumor MDSC-LC.

Impaired MDSC activity in anti–Jagged-treated mice could be a secondary result of direct antitumor effects because smaller tumors may have less MDSC-stimulatory factors. To rule out this, splenic-MDSCs from 3LL-bearing mice were cultured with TES for 48 hours in the presence of anti-Jagged antibody, after which they were cocultured with CFSE-labeled activated T cells. A decreased ability to block T-cell proliferation was noted in the anti–Jagged-treated MDSCs, compared with control MDSCs, which correlated with lower levels of arginase I and iNOS (Fig. 2H and I), suggesting a direct inhibitory effect of the anti-Jagged antibody on tumor-exposed MDSCs.

Anti-Jagged therapy induces antitumor effects through $CD8^+$ T-cell responses

The expansion of MDSCs in tumors is a key driver in the inhibition of protective antitumor T-cell immunity. Thus, we tested the role of $CD8^+$ T cells in the antitumor effects induced by anti-Jagged. Although $CD8^+$ T cells in tumors did not express Jagged1 or 2 (data not shown), we found that treatment of 3LL-bearing mice with anti-Jagged increased the accumulation of $CD8^+$ T cells in tumors (Fig. 3A). Interestingly, anti-Jagged also elevated the proliferation and paradoxically enhanced Notch1 signaling of tumor $CD8^+$ T cells, as suggested by the increased expression of replication marker, Ki-67 (Fig. 3B), and the higher levels of *Notch1* and Notch target gene, *Hes1*, but not *Notch2* (Fig. 3C), respectively. Moreover, elimination of $CD8^+$ T cells partially restored tumor growth in 3LL-bearing mice treated with anti-Jagged (Fig. 3D), confirming the key role of $CD8^+$ T cells in the antitumor effects induced by anti-Jagged. Next, we determined the functional interaction between the anti–Jagged-induced MDSC-LC and $CD8^+$ T cells. Depletion of MDSC-LC prevented the anti–Jagged-induced

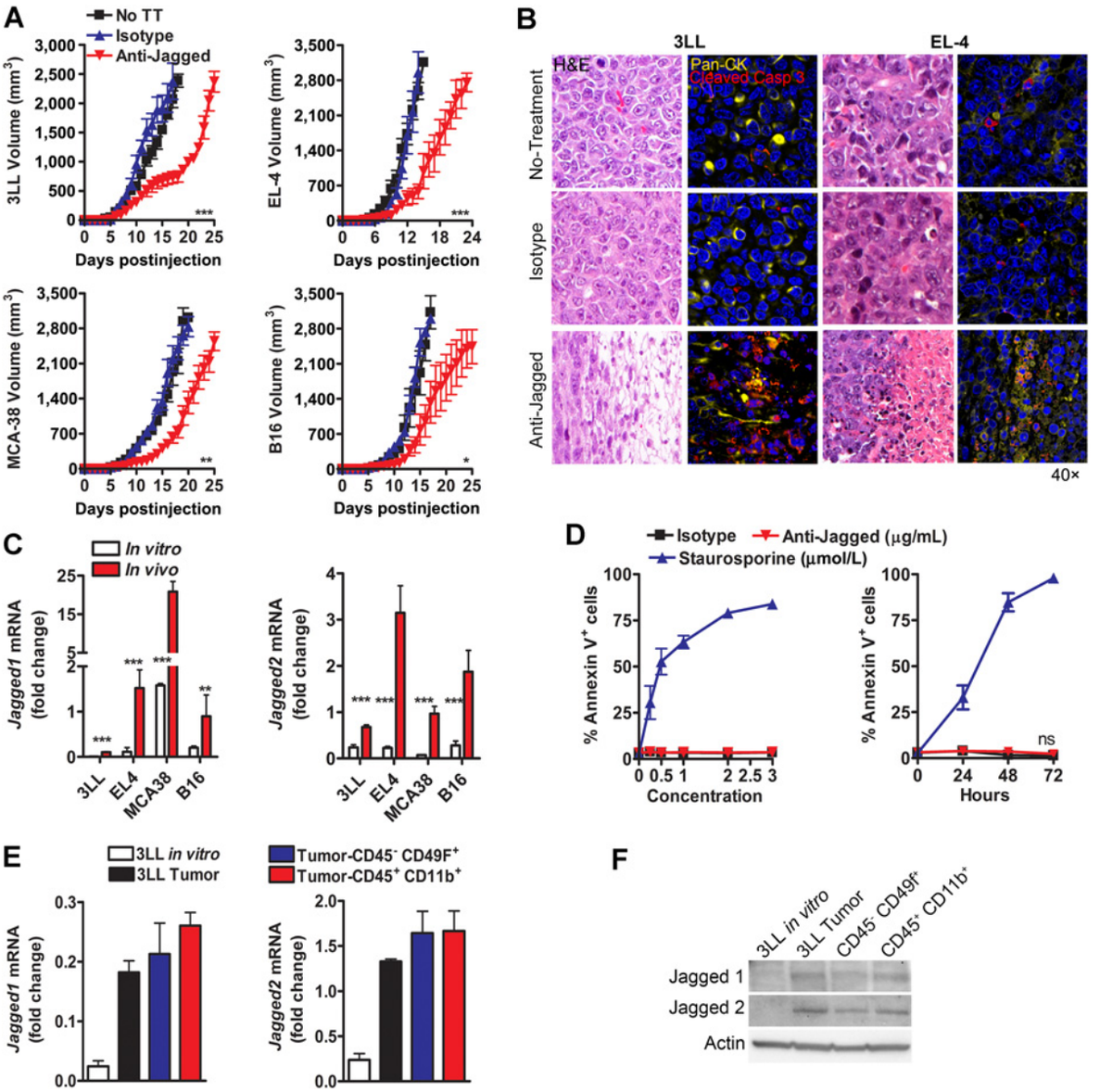

Figure 1.

Anti-Jagged therapy induces antitumor effects. **A,** Tumor volume in mice bearing s.c. 3LL, EL-4, MCA-38, or B16 tumors and treated with anti-Jagged or isotype antibodies, as described in Materials and Methods. Results are mean ± SEM of 15 mice per group. **B,** Tumor morphology by H&E (left) and immunofluorescence against pan-cytokeratin (pan-CK) and cleaved caspase-3 (right) in 3LL- or EL-4–bearing mice treated with anti-Jagged or isotype. Representative images from three repeats. **C,** *Jagged1/2* mRNA by qPCR in 3LL, EL-4, MCA-38, and B16 cells cultured *in vitro* and s.c. tumor suspensions. Data are mean ± SD from three repeats. **D,** The 3LL cells were cultured in the presence of increasing concentrations of anti-Jagged (0–3 ug/ml), isotype (0–3 ug/ml) or the apoptosis inducer staurosporine (0–3 umol/L) for a period of 24 hours (left). In addition, 3LL cells were cultured with anti-Jagged (2 ug/ml), isotype (2 ug/ml), or staurosporine (1 umol/L) for 0–72 hours (right). Then, cells were collected and stained for the expression of Annexin V by flow cytometry. Results are mean of the percentage of Annexin V^+ cells ± SD of three independent repeats. **E** and **F,** Expression of *Jagged1/2* mRNA and protein by qPCR (**E**) or representative Western blot (**F**) in control 3LL cell line and sorted cancer cells ($CD49f^+$ $CD45^{neg}$) and myeloid cells ($CD45^+$ $CD11b^+$) from s.c. 3LL tumors. RNA levels are mean ± SD from 6 mice and tested in triplicates. ***, $P < 0.001$. ns, nonsignificant.

expansion of IFNγ-expressing and antigen-experienced and activated ($CD44^+$ $CD69^+$) $CD8^+$ T cells in tumors (Fig. 3E–G), suggesting that the anti–Jagged-induced MDSC-LC promoted antitumor $CD8^+$ T-cell reactivity.

The expansion of immunogenic $CD11c^+$ $MHC\text{-}II^+$ $CD103^+$ $XCR1^+$ cells has been correlated with development of protective antitumor T-cell immunity (22). An elevated abundance of this cellular subset was noted in 3LL-bearing mice treated with the anti-Jagged therapy (Fig. 3H). However, $CD11c^+$ $MHC\text{-}II^+$ $CD103^+$ $XCR1^+$ cells failed to develop from MDSCs cultured with anti-Jagged, and MDSC-LC were not found in gated immunogenic cells from anti–Jagged-treated mice (Supplementary Fig. S4A and S4B), indicating the independent nature of these populations in mice receiving anti-Jagged.

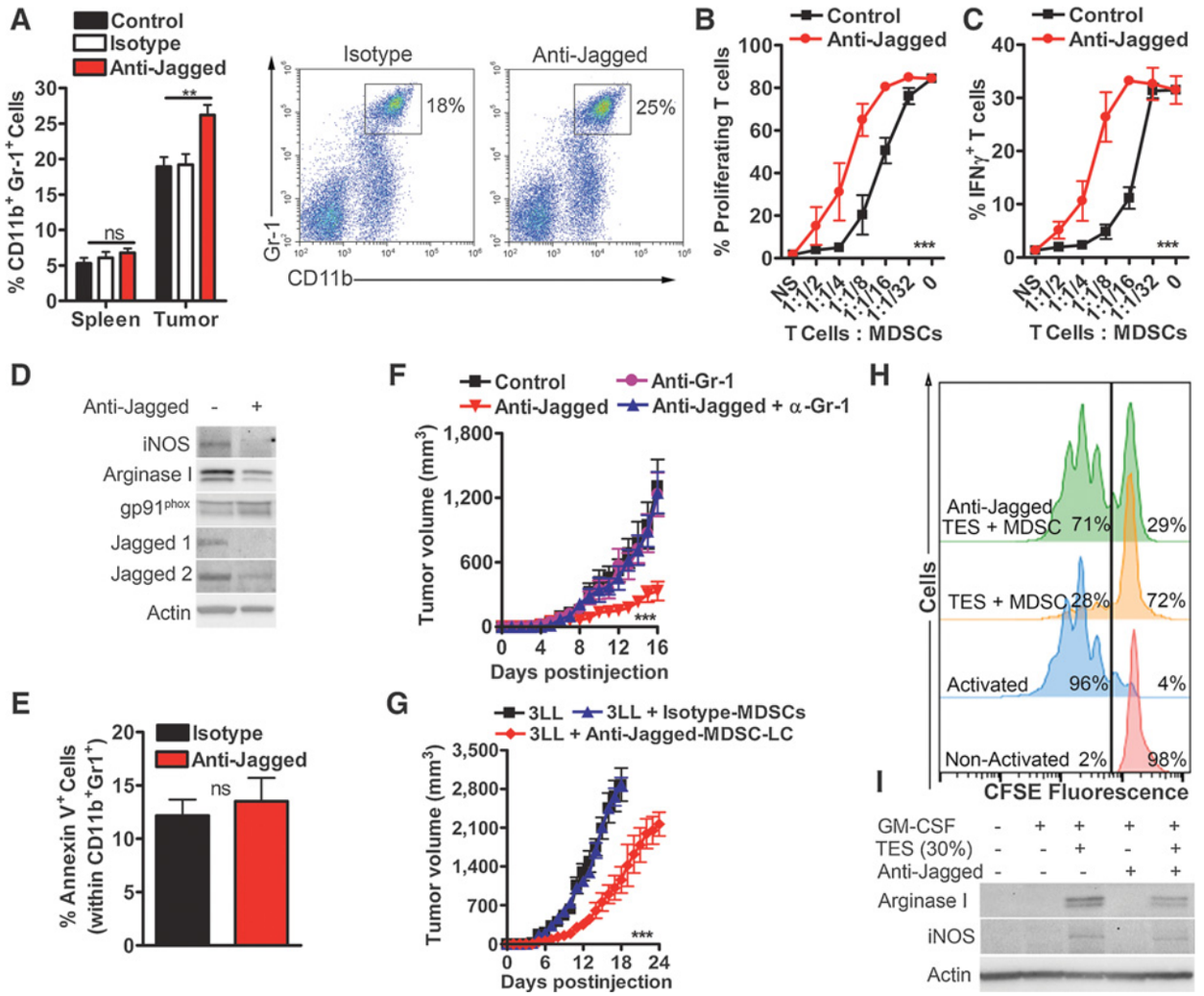

Figure 2.

Anti-Jagged affects the suppressive activity of tumor-MDSC. **A,** Percentages of CD11b$^+$ Gr-1$^+$ cells by flow cytometry in tumor and spleen of 3LL-bearing mice treated with anti-Jagged or isotype. Cumulative data from 10 mice per group (left) and representative results (right). **B** and **C,** Proliferation and IFNγ expression in anti–CD3/CD28-activated CFSE-labeled T cells cocultured for 72 hours with tumor-MDSCs from anti-Jagged or control-treated mice bearing 3LL tumors. Mean ± SD from three experiments. **D,** Western blots from three similar repeats using protein lysates of tumor-MDSCs obtained from mice treated with anti-Jagged or isotype. **E,** Annexin V in MDSCs from **D. F,** Tumor volume in 3LL-bearing mice treated or not with anti-Jagged and receiving anti–Gr-1, as described in Materials and Methods ($n = 5$). **H,** Tumor growth in mice injected with 3LL cells alone or coinjected at a 1:1 ratio with tumor-MDSCs from 3LL-bearing mice treated with anti-Jagged or isotype. Mean ± SEM from 5 mice per group. **H** and **I,** Ability to block proliferation of CFSE-labeled T cells primed with anti-CD3/CD28 and expression of arginase I and iNOS were measured in splenic MDSCs from 3LL-bearing mice cultured for 48 hours in GM-CSF plus 30% TES with and without anti-Jagged. Representative data from three similar experiments. **, $P < 0.01$; ***, $P < 0.001$. ns, nonsignificant.

Anti-Jagged therapy overcomes tumor-induced tolerance and increases the effect of T-cell–based immunotherapy

To address the effect of the anti-Jagged therapy in tumor-induced CD8$^+$ T-cell tolerance, we used an ACT model against the experimental tumor-antigen ovalbumin (OVA), in which activated anti-OVA$_{257\text{-}264}$ (SIINFEKL) transgenic CD45.1$^+$ OT-1 cells were transferred into mice bearing OVA-expressing EG-7 tumors. Anti-Jagged therapy started 6 days after the EG-7 injection, and 1 day later, the mice were transferred with SIINFEKL-preactivated CD45.1$^+$ CD8$^+$ OT-1 cells. A higher antitumor effect was observed in mice treated with anti-Jagged plus ACT, compared with those receiving anti-Jagged or ACT single treatments or untreated controls (Fig. 4A). Accordingly, EG-7–bearing mice treated with anti-Jagged plus ACT had a higher frequency of IFNγ-expressing CD45.1$^+$ CD8$^+$ OT-1 cells in the tumor (Fig. 4B), elevated frequency of clones producing IFNγ upon *ex vivo* activation of splenocytes with SIINFEKL (Fig. 4C), and increased yield of the transferred CD45.1$^+$ OT-1 cells in the tumor and spleen (Fig. 4D and E). A similar effect was found after ACT with nonactivated OT-1 cells (Supplementary Fig. S5A–S5C). Thus, results show the potential benefit of the anti-Jagged therapy as a strategy to overcome tumor-induced T-cell tolerance and as an approach to increase the efficacy of T-cell–based immunotherapy.

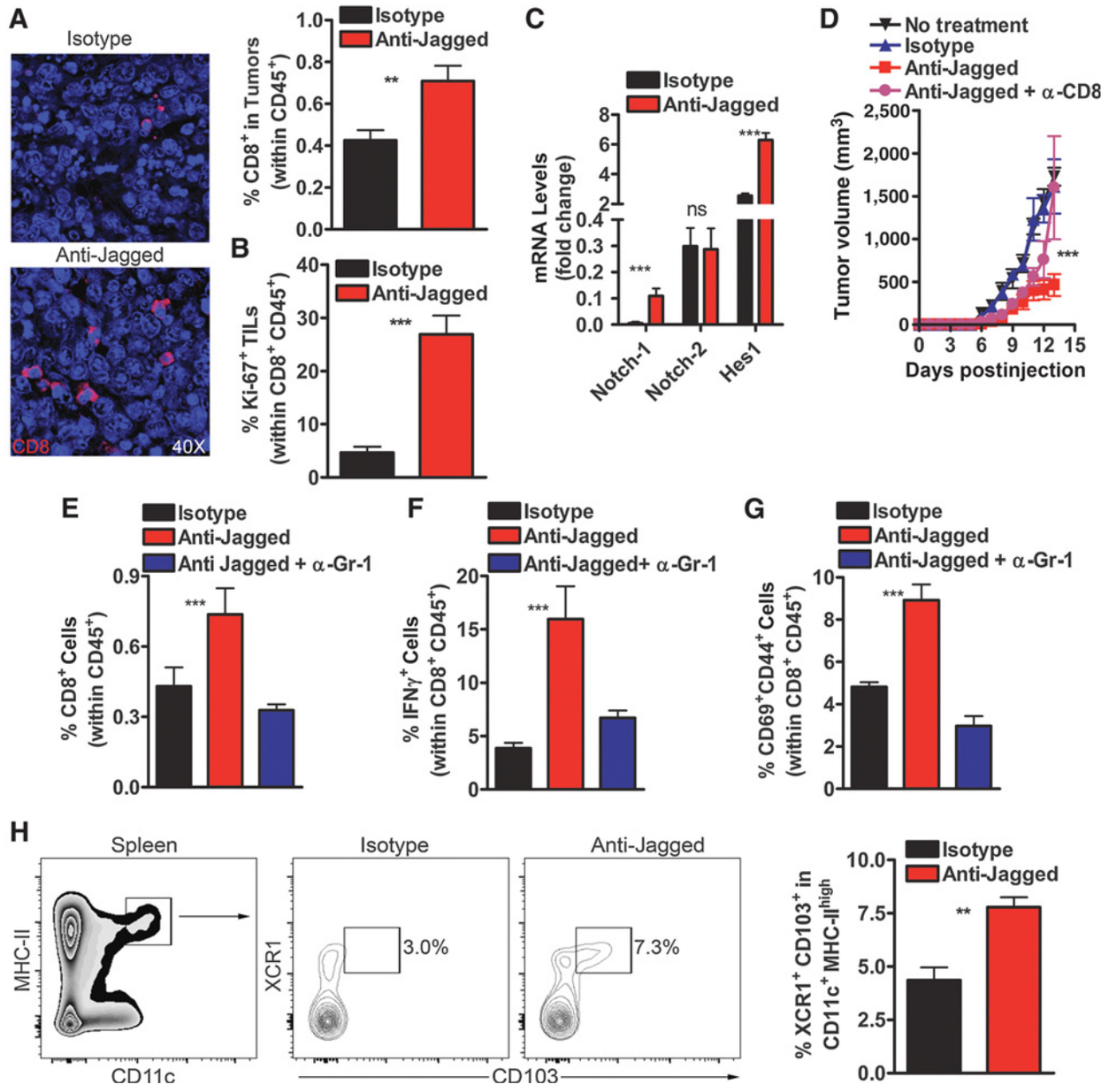

Figure 3.

Antitumor effects induced by anti-Jagged antibody are mediated by $CD8^+$ T cells. **A,** Tumors from 3LL-bearing mice treated with anti-Jagged or control were tested for $CD8^+$ T-cell infiltration by immunofluorescence (left) and flow cytometry (right). Results from five tumors per group. **B,** Percentage of $CD45^+$ $CD8^+$ Ki-67^+ T cells was tested by flow cytometry in tumor suspensions from **A**. **C,** Tumor-associated $CD45^+$ $CD8^+$ T cells were sorted by flow cytometry from 3LL-bearing mice treated with anti-Jagged or control and tested for specific mRNAs using qPCR. **D,** Tumor growth in 3LL-bearing mice treated with anti-Jagged therapy receiving or not anti-CD8 ($n = 5$). **E–G,** Percentage of $CD45^+$ gated $CD8^+$ T cells, IFNγ-producing $CD8^+$ T cells (upon activation with PMA/ionomycin), and $CD44^+$ $CD69^+$ $CD8^+$ T cells in tumors from 3LL-bearing mice treated with anti-Jagged therapy with or without anti–Gr-1. Mean from 5 mice ± SEM. **H,** Spleens from **A** were tested for $CD11C^+$ MHC-II^+ $CD103^+$ $XCR1^+$ cells by flow cytometry. Representative finding (right) and mean of 5 mice ± SEM (left). **, $P < 0.01$; ***, $P < 0.001$. nonsignificant.

During our experiments, we noticed that some of the mice treated with the combination of anti-Jagged and ACT completely rejected the EG-7 tumors. Thus, we studied the potential development of protective memory against the initial tumor. EG-7 cells failed to regrow in mice previously treated with anti-Jagged plus ACT that had rejected the initial tumor, whereas they grew at the usual rate in naïve mice (Fig. 5A and B). Moreover, a partial protection against 3LL tumors was also noted in mice initially treated with anti-Jagged and ACT therapy that had rejected the EG-7 cells (Fig. 5A and B). Thus, combination of anti-Jagged and ACT induced the development of protective immune memory responses against tumors.

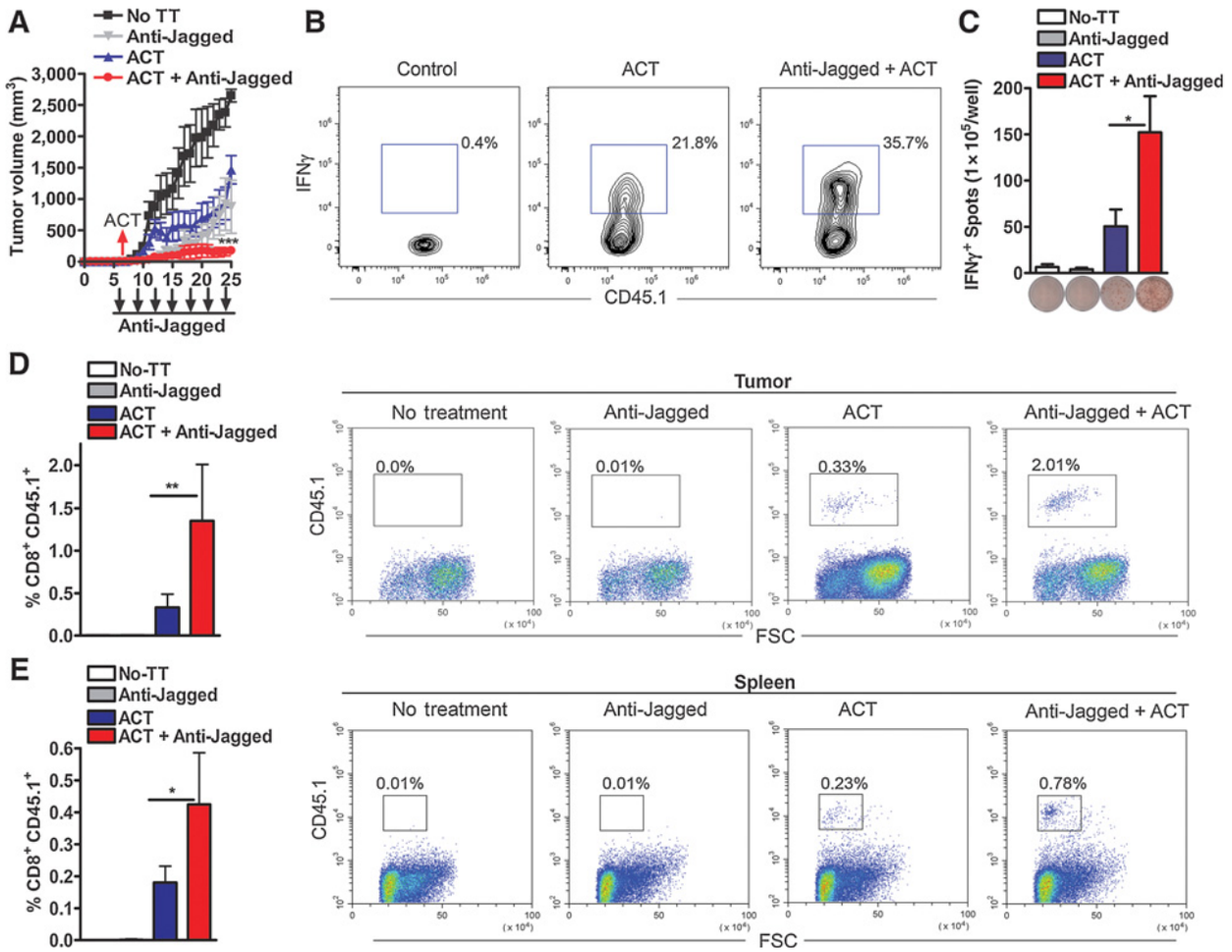

Figure 4.

Jagged blockade overcomes tumor-induced T-cell tolerance and enhances T-cell immunotherapy. **A,** Splenocytes from CD45.1$^+$ OT-1 mice were activated with SIINFEKL (2 μg/mL) for 48 hours, after which CD8$^+$ T cells were negatively sorted and transferred into CD45.2$^+$ mice bearing established EG-7 tumors. Mice received anti-Jagged or transferred T cells alone or in combination of ACT plus anti-Jagged ($n = 10$). **B** and **C,** Ten days after ACT, tumors were activated for 6 hours with PMA/ionomycin, and percentages of IFNγ-producing OT-1 cells were tested by flow cytometry. Spleens were challenged with SIINFEKL and IFNγ production (**B**) measured by Elispot (**C**). Results represent mean ± SD from 5 mice. **D** and **E,** Representative image showing accumulation of CD45.1$^+$ CD8$^+$ T cells in tumor and spleen of mice from **A**. *, $P < 0.05$; **, $P < 0.01$; ***, $P < 0.001$.

Next, we aimed to determine whether the antitumor effect induced after anti-Jagged plus ACT therapy was specifically mediated through the transferred T cells. To test this, ACT alone or anti-Jagged plus ACT therapy was administered to T-cell–deficient Rag mice. Similar to the findings noted in wild-type mice, a significant antitumor effect was found after combination of anti-Jagged and ACT, compared with ACT alone or no treatment controls (Fig. 5C), which correlated with a higher frequency of the transferred CD45.1$^+$ CD8$^+$ OT-1 cells in the tumor (Fig. 5D). Thus, the transferred T cells mediated the antitumor effects induced by anti-Jagged plus ACT.

Tumors induce jagged ligands in MDSCs through NFκB-p65

We aimed to investigate the role of the tumors in the upregulation of Jagged1 and 2 in MDSCs. Increased levels of *Jagged1* and *2* were noted in tumor-infiltrating MDSCs, compared with splenic MDSCs from tumor-bearing mice or iMCs from animals without tumors (Fig. 6A; Supplementary Fig. S6A). To determine the direct influence of tumor factors in the expression of Jagged in MDSCs, splenic MDSCs were cultured in medium containing increasing concentrations of TES. A dose-dependent induction of *Jagged* ligands was found in TES-treated MDSCs, compared with untreated controls (Fig. 6B; Supplementary Fig. S6B). Next, we aimed to identify the intracellular mediators leading to the expression of Jagged1 and 2 in tumor-MDSCs. Activation of NFκB-p65 has been proposed as a common transcription factor regulating MDSC function and Jagged expression (23, 24). Accordingly, we observed elevated nuclear expression of NFκB-p65 in tumor-MDSCs, compared with splenic-MDSCs (Fig. 6C). Also, enhanced endogenous binding of NFκB-p65 to *Jagged1* and *2* promoters was detected in tumor-MDSCs and TES-treated MDSCs (Fig. 6D), compared with control MDSCs, suggesting the direct role of NFκB-p65 in the expression of Jagged1 and 2 in tumor-exposed MDSCs.

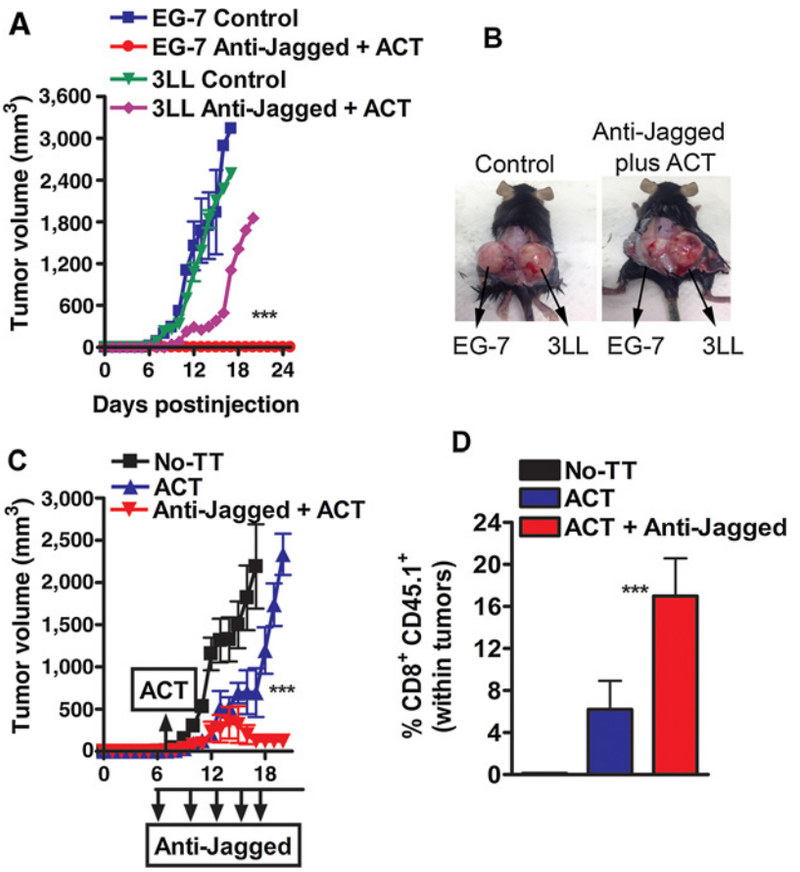

Figure 5.

Anti-Jagged and adoptive T-cell therapy combination induces permanent responses against tumors. **A** and **B,** Mice that were initially treated with anti-Jagged plus ACT therapy and that had completely rejected their tumors were injected with EG-7 (left flank) and 3LL (right flank) and followed for tumor growth ($n = 3$ mice per group). **C,** Tumor volume in immunodeficient Rag-mice bearing established EG-7 tumors that received combination of ACT plus anti-Jagged ($n = 5$ mice per group). **D,** Ten days after ACT, tumors were evaluated for infiltration of CD45.1$^+$ CD8$^+$ OT-1 cells by flow cytometry ($n = 4$ mice per group). ***, $P < 0.001$.

To confirm the role of the NFκB signaling in the induction of Jagged in MDSCs, we used myeloid cell–conditional NFκB-p65 knockout mice (p65^{KO}), which were obtained after crossing floxed p65 mice with LysM-Cre mice. Lower induction of *Jagged* ligands was noted in TES-treated MDSCs and tumor-MDSCs from p65^{KO} mice, compared with LysM-Cre controls (Fig. 7A and B), which also correlated with a significant inability of the p65^{KO} MDSCs to block T-cell proliferation (Fig. 7C). These results show the role of NFκB-p65 in the induction of Jagged1 and 2 in tumor-MDSCs. Next, we tested the antitumor effects of anti-Jagged therapy in p65^{KO} mice. Although anti-Jagged induced significant antitumor responses in LysM-Cre controls, we found similar kinetics of tumor growth in p65^{KO} mice treated with anti-Jagged or isotype (Fig. 7D), indicating the potential role of the NFκB-p65–dependent upregulation of Jagged in MDSCs as a target for anti-Jagged therapy.

Discussion

In this study, we aimed to test the efficacy of the Jagged1/2-blocking antibody, CTX014, in tumor-bearing mice. The results characterize a promising therapeutic tool to reprogram MDSC-mediated T-cell suppression in tumors, thereby addressing a major obstacle in the development of successful therapies against cancer. Findings also advance in the understanding of the role of Notch ligands as primary modulators of tumor-associated immune responses.

Accumulating evidence indicates the opposite effects of the activation of Notch in T cells through DLL or Jagged ligands. DLL1 and 4 induced development of Th1 cells and effector memory CD8$^+$ T cells (15, 25–29), whereas Jagged1 and 2 skewed T cells into Th2, Treg, and anergic CD8$^+$ T populations (16, 30–33). In agreement with the proposed immune inhibitory role of Jagged, we found that anti-Jagged overcame tumor T-cell suppression through the induction of potentially immunogenic MDSC-LC. Our data also showed the expression of Jagged ligands in cancer cells and tumor-myeloid cells. Although anti-Jagged directly modulated MDSC function in *vitro*, it remains unknown whether the induced antitumor effects are a combination of Jagged targeting on cancer cells and MDSCs. In fact, it is possible that direct effects of anti-Jagged on tumor cells could result in immunogenic cell death–related responses promoting MDSC-LC. Thus, differential modulation of Jagged forms in cancer cells versus myeloid cells will allow us to test the contribution of Jagged on these subsets in the inhibition of antitumor immunity. Also, understanding of the mechanisms of action of the anti-Jagged antibody, including the role of complement activation, antibody-dependent cell-mediated cytotoxicity, and antibody-dependent cellular phagocytosis will better characterize the mediators for this therapy in cancer.

Inhibition of Notch signaling in T cells is emerging as a major mechanism of immune evasion in tumors. However, the pathways blunting Notch activity in T cells remain unclear. MDSCs blocked the induction of full-length and cleaved Notch in T cells

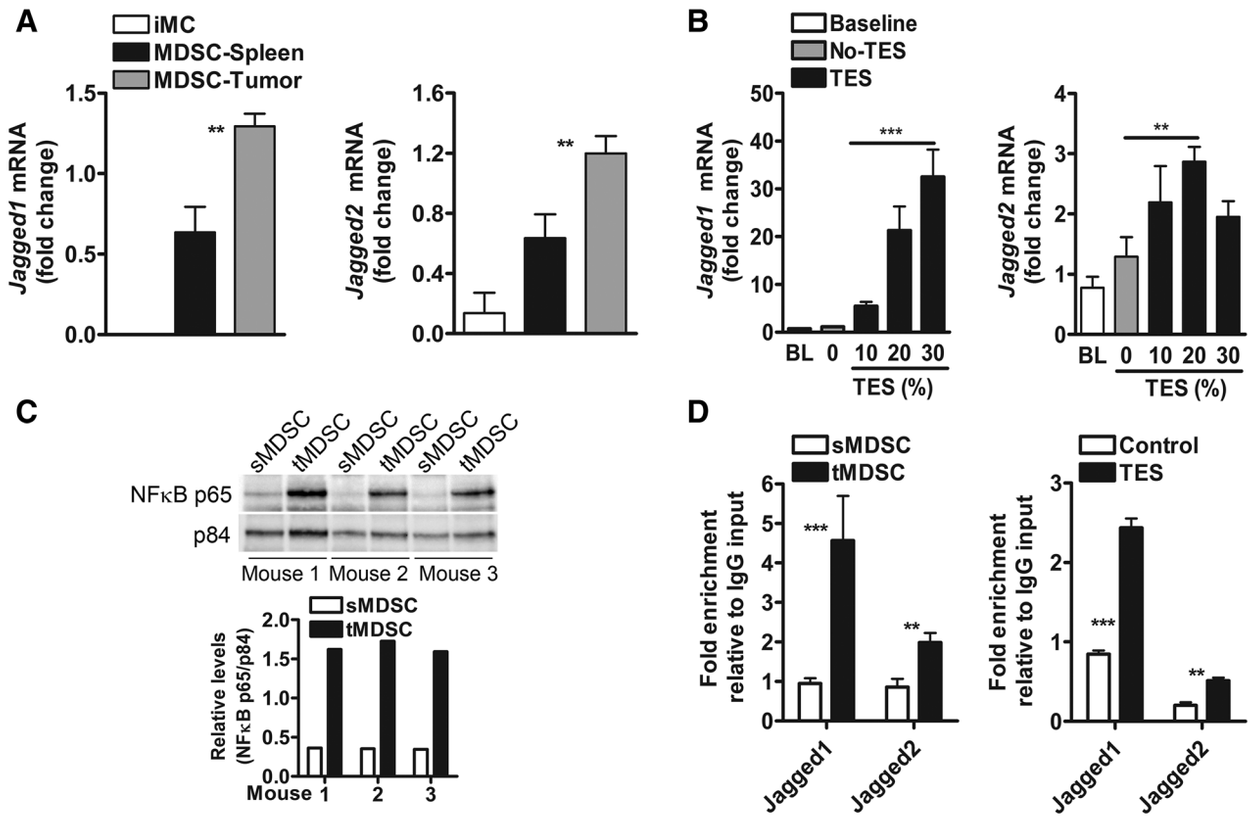

Figure 6.

Tumor-induced NFκB-p65 drives the expression of Jagged ligands in tumor MDSC. **A,** *Jagged1* and *2* mRNA in tumor and splenic MDSCs from mice bearing 3LL tumors and in iMC from mice without tumors. Data represent mean ± SD of five samples from different mice. **B,** *Jagged1* and *2* mRNA in splenic MDSCs from 3LL-bearing mice cultured for 48 hours in GM-CSF–containing medium supplemented with increasing levels of TES. Results are from three independent experiments. **C,** NFκB-p65 in nuclear extracts from tumor and splenic MDSCs sorted from 3LL-bearing mice. A representative result from three repeats. **D,** ChIP assays to detect the endogenous binding of NFκB-p65 to Jagged1 and 2 promoters were assessed in cells from **C**. Results represent mean ± SD from two experiments. **, $P < 0.01$; ***, $P < 0.001$.

through nitric oxide–dependent pathways (14). Also, the impaired Notch activity found in T cells from tumor-bearing hosts was rescued by the proteasome inhibitor bortezomib, suggesting the posttranslational regulation of T-cell-Notch in tumors (34). Additional data showed that methylation of the Notch regulator, Numb, triggered Notch activity upon T-cell stimulation, indicating the epigenetic regulation of Notch signaling in T cells (35). Because impaired Notch activity in T cells blocks their antitumor potential, it is conceivable that restoring T-cell-Notch signaling could promote antitumor immunity. Indeed, ectopic expression of NICD rendered $CD8^+$ T cells less susceptible to the regulatory effects of tumors and increased their efficacy upon ACT (14). Moreover, activation of T-cell-Notch through a DLL1–Fc fusion complex induced central memory $CD8^+$ T cells that had heightened antitumor effects (15, 36). Accordingly, systemic DLL1 delivery promoted T-cell infiltration into tumors and enhanced efficacy of EGFR-targeted therapy (36). Collectively, these studies show that activation of DLL-Notch signaling could represent an opportunity to restore $CD8^+$ T-cell responses in tumors. Interestingly, we found a paradoxical elevation of Notch1 signaling in tumor-linked $CD8^+$ T cells from anti–Jagged-treated mice. This effect could be explained by the induction of MDSC-LC with impaired regulatory function that fails to block Notch1 in T cells. An additional possibility is that reprogramming of MDSCs by anti-Jagged could lead to the induction of DLL1 and 4, which induce Notch activation in T cells. The specific role of these possibilities is currently under investigation.

Similar to T cells, DLL and Jagged ligands induced opposite effects in myeloid cells. Myeloid precursors cultured with fibroblasts expressing DLL1 differentiated into functional DCs, whereas activation of Notch through Jagged promoted immature myeloid cells (37) and induced IL10 (38). A potential explanation for the opposite roles of DLL and Jagged in myeloid cells is their differential effects on Wnt pathway (39, 40). Our data show that tumor-derived factors trigger the expression of Jagged1/2 in tumor-associated MDSCs through NFκB-p65. However, the tumor factors increasing NFκB signaling remain unknown. Potential mediators include TNFα and IL1β, both highly elevated in most tumor microenvironments and key regulators of MDSC function (41, 42). Additional candidates include the exposure of MDSCs to hypoxia, tumor exosomes, or S100A8/A9 (43–45). In addition to inducing Jagged, NFκB controls the production of several cytokines, including IL6, IL10, TNFα, and IL1β, which occurs not only by direct NFκB transcriptional activity, but also through partnering

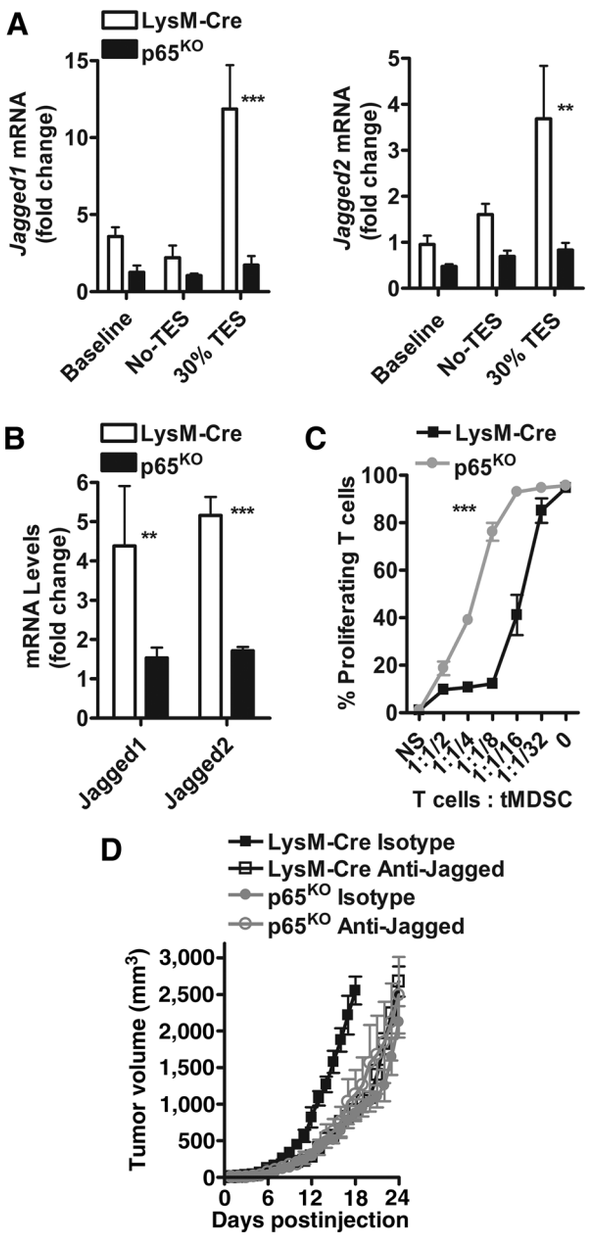

Figure 7.

Deletion of NFκB-p65 decreases Jagged1 and 2 expression and blocks MDSC suppression in tumors. **A,** Splenic MDSCs harvested from LysM-Cre controls and myeloid cell–conditional NFκB-p65^{KO} mice bearing similar-sized 3LL tumors were cultured in the presence of 30% TES for 48 hours, after which the levels of *Jagged1* and *2* mRNA were tested by qPCR. Data are mean ± SD from three repeats. **B,** *Jagged1* and *2* mRNA levels in tumor-MDSCs collected from LysM-Cre controls and myeloid cell–conditional NFκB-p65^{KO} mice bearing 3LL tumors. Mean ± SD from five different tumors. **C,** Immunosuppressive activity of MDSCs from **B** against CFSE-labeled T cells stimulated with anti-CD3/CD28. Percentages of proliferating T cells were measured at 72 hours by flow cytometry. Results are mean ± SD from three repeats. **D,** Tumor volume in NFκB-p65^{KO} and LysM-Cre mice bearing 3LL tumors and treated or not with anti-Jagged ($n = 5$). **, $P < 0.01$ and ***, $P < 0.001$.

with other factors, including Notch, hypoxia-inducible factor alpha, and the activator of transcription 3 (46–50).

In summary, our study describes a new therapeutic strategy to overcome MDSC-mediated T-cell suppression in tumors, which could increase the efficacy of several cancer treatments, such as T-cell–based immunotherapies that remain highly limited by the regulatory action of MDSCs.

Disclosure of Potential Conflicts of Interest

No potential conflicts of interest were disclosed.

Authors' Contributions

Conception and design: R.A. Sierra, L. Yu, L. Miele, P.C. Rodriguez
Development of methodology: R.A. Sierra
Acquisition of data (provided animals, acquired and managed patients, provided facilities, etc.): R.A. Sierra, J. Trillo-Tinoco, L. Yu, B.R. Achyut, A. Arbab, J.W. Bradford
Analysis and interpretation of data (e.g., statistical analysis, biostatistics, computational analysis): R.A. Sierra, J. Trillo-Tinoco, E. Mohamed, L. Miele, P.C. Rodriguez
Writing, review, and/or revision of the manuscript: R.A. Sierra, J. Trillo-Tinoco, E. Mohamed, L. Yu, A. Arbab, J.W. Bradford, B.A. Osborne, L. Miele, P.C. Rodriguez
Administrative, technical, or material support (i.e., reporting or organizing data, constructing databases): R.A. Sierra, B.R. Achyut, P.C. Rodriguez
Study supervision: R.A. Sierra, P.C. Rodriguez
Other (I am not the senior author. The senior author is Dr. Rodriguez): L. Yu

Acknowledgments

We would like to thank CytomX for providing the anti-Jagged antibody.

Grant Support

This work was partially supported by NIH-CA184185 to P.C. Rodriguez and by a pilot program from CytomX to P.C. Rodriguez and L. Miele.

The costs of publication of this article were defrayed in part by the payment of page charges. This article must therefore be hereby marked *advertisement* in accordance with 18 U.S.C. Section 1734 solely to indicate this fact.

Received February 7, 2017; revised June 17, 2017; accepted August 23, 2017; published OnlineFirst September 13, 2017.

References

1. Speiser DE, Ho PC, Verdeil G. Regulatory circuits of T cell function in cancer. Nat Rev Immunol 2016;16:599–611.
2. Gabrilovich DI, Ostrand-Rosenberg S, Bronte V. Coordinated regulation of myeloid cells by tumours. Nat Rev Immunol 2012;12:253–68.
3. Ko JS, Zea AH, Rini BI, Ireland JL, Elson P, Cohen P, et al. Sunitinib mediates reversal of myeloid-derived suppressor cell accumulation in renal cell carcinoma patients. Clin Cancer Res 2009;15:2148–57.
4. Bruchard M, Mignot G, Derangere V, Chalmin F, Chevriaux A, Vegran F, et al. Chemotherapy-triggered cathepsin B release in myeloid-derived suppressor cells activates the Nlrp3 inflammasome and promotes tumor growth. Nat Med 2013;19:57–64.
5. Weiner LM, Murray JC, Shuptrine CW. Antibody-based immunotherapy of cancer. Cell 2012;148:1081–4.
6. Scott AM, Wolchok JD, Old LJ. Antibody therapy of cancer. Nat Rev Cancer 2012;12:278–87.
7. Dominguez GA, Condamine T, Mony S, Hashimoto A, Wang F, Liu Q, et al. Selective targeting of myeloid-derived suppressor cells in cancer patients using DS-8273a, an agonistic TRAIL-R2 antibody. Clin Cancer Res 2017;23:2942–50.
8. Radtke F, MacDonald HR, Tacchini-Cottier F. Regulation of innate and adaptive immunity by Notch. Nat Rev Immunol 2013;13:427–37.
9. Guruharsha KG, Kankel MW, rtavanis-Tsakonas S. The Notch signalling system: recent insights into the complexity of a conserved pathway. Nat Rev Genet 2012;13:654–66.

10. Radtke F, Fasnacht N, MacDonald HR. Notch signaling in the immune system. Immunity 2010;32:14–27.
11. Osborne BA, Minter LM. Notch signalling during peripheral T-cell activation and differentiation. Nat Rev Immunol 2007;7:64–75.
12. Minter LM, Osborne BA. Canonical and non-canonical Notch signaling in CD4(+) T cells. Curr Top Microbiol Immunol 2012;360:99–114.
13. Sugimoto K, Maekawa Y, Kitamura A, Nishida J, Koyanagi A, Yagita H, et al. Notch2 signaling is required for potent antitumor immunity in vivo. J Immunol 2010;184:4673–78.
14. Sierra RA, Thevenot P, Raber PL, Cui Y, Parsons C, Ochoa AC, et al. Rescue of notch-1 signaling in antigen-specific CD8+ T cells overcomes tumor-induced T-cell suppression and enhances immunotherapy in cancer. Cancer Immunol Res 2014;2:800–11.
15. Huang Y, Lin L, Shanker A, Malhotra A, Yang L, Dikov MM, et al. Resuscitating cancer immunosurveillance: selective stimulation of DLL1-Notch signaling in T cells rescues T-cell function and inhibits tumor growth. Cancer Res 2011;71:6122–31.
16. Kijima M, Iwata A, Maekawa Y, Uehara H, Izumi K, Kitamura A, et al. Jagged1 suppresses collagen-induced arthritis by indirectly providing a negative signal in CD8+ T cells. JImmunol 2009;182:3566–72.
17. Bronte V, Brandau S, Chen SH, Colombo MP, Frey AB, Greten TF, et al. Recommendations for myeloid-derived suppressor cell nomenclature and characterization standards. Nat Commun 2016;7:12150.
18. Thevenot PT, Sierra RA, Raber PL, Al-Khami AA, Trillo-Tinoco J, Zarreii P, et al. The stress-response sensor chop regulates the function and accumulation of myeloid-derived suppressor cells in tumors. Immunity 2014;41:389–401.
19. Steinbrecher KA, Harmel-Laws E, Sitcheran R, Baldwin AS. Loss of epithelial RelA results in deregulated intestinal proliferative/apoptotic homeostasis and susceptibility to inflammation. J Immunol 2008;180: 2588–99.
20. Raber PL, Thevenot P, Sierra R, Wyczechowska D, Halle D, Ramirez ME, et al. Subpopulations of myeloid-derived suppressor cells impair T cell responses through independent nitric oxide-related pathways. Int J Cancer 2014;134:2853–64.
21. Hossain F, Al-Khami AA, Wyczechowska D, Hernandez C, Zheng L, Reiss K, et al. Inhibition of fatty acid oxidation modulates immunosuppressive functions of myeloid-derived suppressor cells and enhances cancer therapies. Cancer Immunol Res 2015;3:1236–47.
22. Zelenay S, van der Veen AG, Bottcher JP, Snelgrove KJ, Rogers N, Acton SE, et al. Cyclooxygenase-dependent tumor growth through evasion of immunity. Cell 2015;162:1257–70.
23. Johnston DA, Dong B, Hughes CC. TNF induction of jagged-1 in endothelial cells is NFkappaB-dependent. Gene 2009;435:36–44.
24. Hu X, Li B, Li X, Zhao X, Wan L, Lin G, et al. Transmembrane TNF-alpha promotes suppressive activities of myeloid-derived suppressor cells via TNFR2. J Immunol 2014;192:1320–31.
25. Meng L, Bai Z, He S, Mochizuki K, Liu Y, Purushe J, et al. The notch ligand DLL4 defines a capability of human dendritic cells in regulating Th1 and Th17 differentiation. J Immunol 2016;196:1070–80.
26. Backer RA, Helbig C, Gentek R, Kent A, Laidlaw BJ, Dominguez CX, et al. A central role for Notch in effector CD8(+) T cell differentiation. NatImmunol 2014;15:1143–51.
27. Skokos D, Nussenzweig MC. CD8- DCs induce IL-12-independent Th1 differentiation through Delta 4 Notch-like ligand in response to bacterial LPS. J Exp Med 2007;204:1525–31.
28. Backer RA, Helbig C, Gentek R, Kent A, Laidlaw BJ, Dominguez CX, et al. A central role for Notch in effector CD8(+) T cell differentiation. Nat Immunol 2014;15:1143–51.
29. Mathieu M, Duval F, Daudelin JF, Labrecque N. The Notch signaling pathway controls short-lived effector CD8+ T cell differentiation but is dispensable for memory generation. J Immunol 2015;194:5654–62.
30. Amsen D, Antov A, Flavell RA. The different faces of Notch in T-helper-cell differentiation. Nat Rev Immunol 2009;9:116–24.
31. Amsen D, Antov A, Jankovic D, Sher A, Radtke F, Souabni A, et al. Direct regulation of Gata3 expression determines the T helper differentiation potential of Notch. Immunity 2007;27:89–99.
32. Tu L, Fang TC, Artis D, Shestova O, Pross SE, Maillard I, et al. Notch signaling is an important regulator of type 2 immunity. J Exp Med 2005; 202:1037–42.
33. Auderset F, Schuster S, Coutaz M, Koch U, Desgranges F, Merck E, et al. Redundant Notch1 and Notch2 signaling is necessary for IFNgamma secretion by T helper 1 cells during infection with Leishmania major. PLoS Pathog 2012;8:e1002560.
34. Thounaojam MC, Dudimah DF, Pellom ST Jr., Uzhachenko RV, Carbone DP, Dikov MM, et al. Bortezomib enhances expression of effector molecules in anti-tumor CD8+ T lymphocytes by promoting Notch-nuclear factor-kappaB crosstalk. Oncotarget 2015;6:32439–55.
35. Zhao E, Maj T, Kryczek I, Li W, Wu K, Zhao L, et al. Cancer mediates effector T cell dysfunction by targeting microRNAs and EZH2 via glycolysis restriction. Nat Immunol 2016;17:95–103.
36. Biktasova AK, Dudimah DF, Uzhachenko RV, Park K, Akhter A, Arasada RR, et al. Multivalent forms of the notch ligand DLL-1 enhance antitumor T-cell immunity in lung cancer and improve efficacy of EGFR-targeted therapy. Cancer Res 2015;75:4728–41.
37. Cheng P, Nefedova Y, Corzo CA, Gabrilovich DI. Regulation of dendritic-cell differentiation by bone marrow stroma via different Notch ligands. Blood 2007;109:507–15.
38. Bugeon L, Gardner LM, Rose A, Gentle M, Dallman MJ. Cutting edge: Notch signaling induces a distinct cytokine profile in dendritic cells that supports T cell-mediated regulation and IL-2-dependent IL-17 production. J Immunol 2008;181:8189–93.
39. Liu H, Zhou J, Cheng P, Ramachandran I, Nefedova Y, Gabrilovich DI. Regulation of dendritic cell differentiation in bone marrow during emergency myelopoiesis. J Immunol 2013;191:1916–26.
40. Zhou J, Cheng P, Youn JI, Cotter MJ, Gabrilovich DI. Notch and wingless signaling cooperate in regulation of dendritic cell differentiation. Immunity 2009;30:845–59.
41. Tu S, Bhagat G, Cui G, Takaishi S, Kurt-Jones EA, Rickman B, et al. Overexpression of interleukin-1beta induces gastric inflammation and cancer and mobilizes myeloid-derived suppressor cells in mice. Cancer Cell 2008;14:408–19.
42. Zhao X, Rong L, Zhao X, Li X, Liu X, Deng J, et al. TNF signaling drives myeloid-derived suppressor cell accumulation. J Clin Invest 2012;122: 4094–104.
43. Liu Y, Xiang X, Zhuang X, Zhang S, Liu C, Cheng Z, et al. Contribution of MyD88 to the tumor exosome-mediated induction of myeloid derived suppressor cells. Am J Pathol 2010;176:2490–9.
44. Corzo CA, Condamine T, Lu L, Cotter MJ, Youn JI, Cheng P, et al. HIF-1alpha regulates function and differentiation of myeloid-derived suppressor cells in the tumor microenvironment. J Exp Med 2010;207:2439–53.
45. Sinha P, Okoro C, Foell D, Freeze HH, Ostrand-Rosenberg S, Srikrishna G. Proinflammatory S100 proteins regulate the accumulation of myeloid-derived suppressor cells. J Immunol 2008;181:4666–75.
46. Osipo C, Golde TE, Osborne BA, Miele LA. Off the beaten pathway: the complex cross talk between Notch and NF-kappaB. Lab Invest 2008;88: 11–7.
47. Aguilera C, Hoya-Arias R, Haegeman G, Espinosa L, Bigas A. Recruitment of IkappaBalpha to the hes1 promoter is associated with transcriptional repression. Proc Natl Acad Sci U S A 2004;101:16537–42.
48. Nefedova Y, Cheng P, Gilkes D, Blaskovich M, Beg AA, Sebti SM, et al. Activation of dendritic cells via inhibition of Jak2/STAT3 signaling. J Immunol 2005;175:4338–46.
49. Kusmartsev S, Nefedova Y, Yoder D, Gabrilovich DI. Antigen-specific inhibition of CD8+ T cell response by immature myeloid cells in cancer is mediated by reactive oxygen species. J Immunol 2004;172:989–99.
50. Mancino A, Lawrence T. Nuclear factor-kappaB and tumor-associated macrophages. Clin Cancer Res 2010;16:784–9.